# *Magnetic Nanodrug Delivery Through the Mucus Layer of Air-Liquid Interface Cultured Primary Normal Human Tracheobronchial Epithelial Cells*

**E. C. Economou, S. Marinelli, M. C. Smith, A. A. Routt, V. V. Kravets, H. W. Chu, K. Spendier & Z. J. Celinski**

**BioNanoScience**

ISSN 2191-1630

BioNanoSci.
DOI 10.1007/s12668-016-0216-y

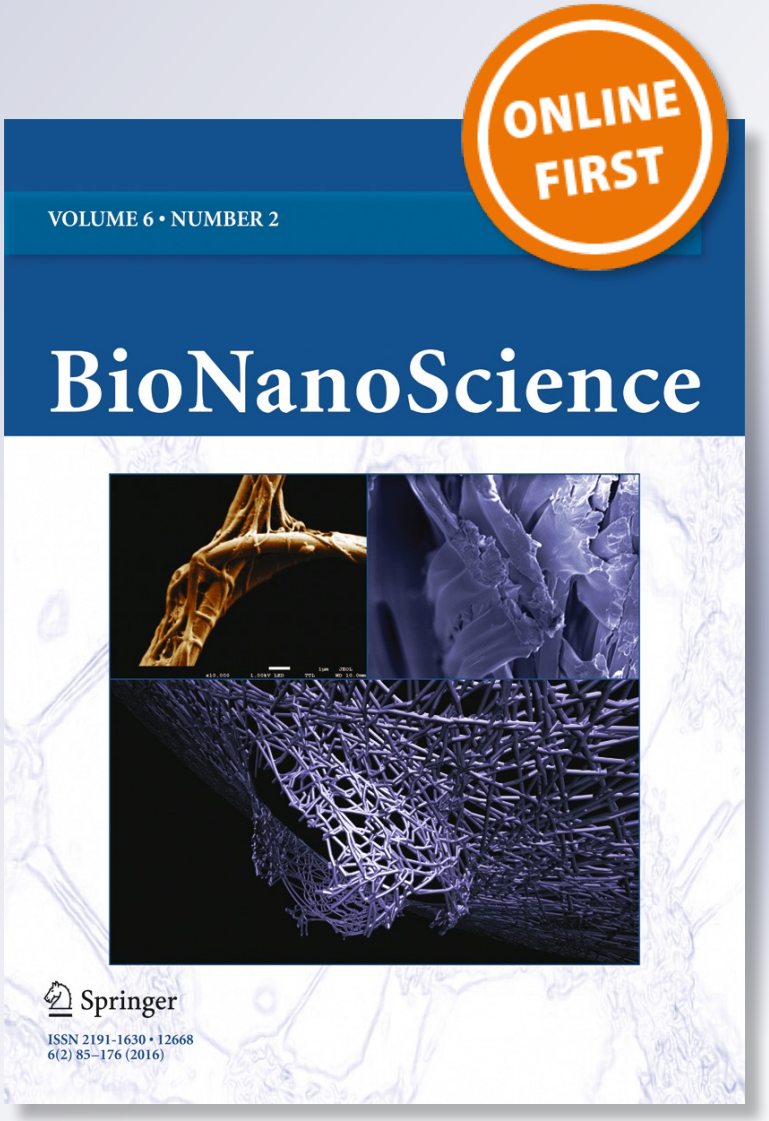


Springer

BioNanoSci.
DOI 10.1007/s12668-016-0216-y

# Magnetic Nanodrug Delivery Through the Mucus Layer of Air-Liquid Interface Cultured Primary Normal Human Tracheobronchial Epithelial Cells

**E. C. Economou [1,2] · S. Marinelli [1] · M. C. Smith [1] · A. A. Routt [1] · V. V. Kravets [1,2] · H. W. Chu [3] · K. Spendier [1,2] · Z. J. Celinski [1,2]**



**Abstract** Superparamagnetic iron oxide ($Fe_3O_4$) and highly anisotropic barium hexaferrite ($BaFe_{12}O_{19}$) nanoparticles were coated with an anti-inflammatory drug and magnetically transported through mucus produced by primary human airway epithelial cells. Using wet planetary ball milling, DL-2-amino-3-phosphonopropionic acid-coated $BaFe_{12}O_{19}$ nanoparticles (BaNPs) of 1–100 nm in diameter were prepared in water. BaNPs and conventional 20–30-nm $Fe_3O_4$ nanoparticles (FeNPs) were then encased in a polymer (PLGA) loaded with dexamethasone (Dex) and tagged for imaging. PLGA-Dex-coated BaNPs and FeNPs were characterized using dynamic light scattering (DLS), transmission electron microscopy (TEM), and superconducting quantum interference device (SQUID) magnetometry. Both PLGA-Dex-coated BaNPs and FeNPs were transferred to the surface of a ~100-μm thick mucus layer of air-liquid interface cultured primary normal human tracheobronchial epithelial (NHTE) cells. Within 30 min, the nanoparticles were pulled successfully through the mucus layer by a permanent neodymium magnet. The penetration time of the nanomedicine was monitored using confocal microscopy and tailored by varying the thickness of the PLGA-Dex coating around the particles.

**Keywords** High anisotropy magnetic nanoparticles · Barium hexaferrite · Dexamethasone · Drug delivery · Mucus overproduction · Nanotherapeutics · Nanomedicine

## 1 Introduction

Excessive mucus production is a common and significant problem for several prominent human lung diseases such as asthma and chronic obstructive pulmonary disease (COPD). Treatment of these lung diseases typically focuses on reduction or elimination of mucus, bacterial and viral infections, and inflammation. However, therapeutic efficacy of many drugs remains poor due to a thick mucus layer which poses a significant challenge to drug delivery.

To date, there is no effective therapy for excessive airway mucus. Because inflammation is a key contributor to mucus production, various anti-inflammatory drugs such as corticosteroids (CS) have been used to inhibit mucus both in vitro (airway epithelial cell culture model) and in vivo [1, 2]. However, a large number of asthmatics receiving CS continue to produce mucus, suggesting a limited in vivo therapeutic effect of CS [3].

Because of the poor efficacy of current anti-mucus therapy, new approaches such as the use of nanoparticles (NPs) are being investigated. One of the major therapeutic challenges in lung diseases is to overcome the obstructive barrier of respiratory mucus that hinders nanodelivery to the diseased epithelium. For a nanotherapeutic to safely pass across the mucus barrier, researchers have modified both NP size and surface properties. NPs coated with biocompatible polymers such as polyethylene glycol (PEG) can move quickly through mouse cervicovaginal mucus (~100-μm layer) [4]. Although PEGylated polystyrene NPs enhance penetration in model systems, sputa of cystic fibrosis patients [5] and fresh

✉ E. C. Economou
eeconomo@uccs.edu

[1] Center of the BioFrontiers Institute, University of Colorado at Colorado Springs, 1420 Austin Bluffs Parkway, Colorado Springs, CO 80918, USA

[2] Department of Physics and Energy Science, University of Colorado at Colorado Springs, Colorado Springs, CO 80918, USA

[3] Department of Medicine, National Jewish Health, Denver, CO 80206, USA

Published online: 28 July 2016

undiluted mucus [6], it is unknown if such mucus-penetrating NPs withstand the rapid mucus clearance (7–14 mm/min) [7].

To overcome mucus clearance and guide nanotherapeutics through the mucus barrier, NPs with magnetic cores have been employed. In this strategy, magnetic NPs are pulled by external magnetic forces through the mucosal barrier. For example, superparamagnetic $Fe_3O_4$ NPs (FeNPs) enhance diffusion through model mucus using spatial-varying magnetic field gradient guiding in vitro [8]. However, in an ex vivo bullfrog (*Rana catesbeiana*) palate model that was intended to simulate the airway surface with typical mucus transport velocities, magnetic FeNPs could not penetrate the mucus in a static magnetic field gradient of 10 T/m [9]. Moreover, Kirch et al. showed that magnetic FeNPs could not be pulled through human respiratory mucus in a static magnetic field [10]. The authors concluded that a rigid gel scaffold in lung mucus separates large, fluid-filled pores preventing magnetic FeNP movement beyond individual pore boundaries.

Based on these previous studies showing no mucus penetration, a spatial-varying magnetic field gradient of 10 T/m may not be sufficient for pulling magnetic NPs through mucus. Therefore, in our study, a permanent neodymium (NdFeB) magnet with an iron core pole piece was used to generate a high field gradient of 295 ± 15 T/m at the pole piece tip in order to produce an order of magnitude stronger pulling force than in previously applied FeNP delivery systems for mucus penetration. A similar system with a tip architecture using an electromagnet produced a slightly lower field gradient of 150 T/m at the tip [11]. In this study, it was shown that FeNP aerosol droplets can be delivered to regions of the mouse lung, but mucus penetration was not demonstrated. Using a field gradient of 60 ± 3 T/m (2.5 mm above the tip), we successfully pulled anti-inflammation drug (i.e., Dex)-coated FeNPs through the mucus layer of air-liquid interface (ALI)-cultured primary normal human tracheobronchial epithelial (NHTE) cells for the first time. Furthermore, the penetration of drug-coated barium hexaferrite nanoparticles (BaNPs) was also demonstrated. BaNPs have a potential advantage over the conventional FeNP technology since barium hexagonal ferrites have five times larger magnetic anisotropy [12].

## 2 Materials and Methods

### 2.1 Fabrication of Functionalized $BaFe_{12}O_{19}$ Nanoparticles

Wet planetary ball milling was used to prepare BaNPs for drug-coating [13]. The final size of the NPs after milling is primarily a function of the milling time, revolutions per minute (RPM), and quantity and type of grinding balls and chemicals. Here, the milling time was varied, while other factors were held constant. The materials for the milling phase include powdered $BaFe_{12}O_{19}$ (500-nm average diameter, polyhedral-shaped) from Nanostructured and Amorphous Materials, Inc., DL-2-amino-3-phosphonopropionic acid (AP3, 169.07 M.W.) from Sigma-Aldrich, and double distilled water ($ddH_2O$, 18.2 MΩ/cm). AP3 is derivatized with a phosphoric group, which utilizes covalent bonding for surface functionalization of metal oxides [14]. Besides its compatibility with metal oxides, it also acts as a heterobifunctional coupling agent for the PLGA-Dex coating. Furthermore, AP3 allows the particles to disperse well in water.

An amount of 0.405 g of powdered $BaFe_{12}O_{19}$, 0.078 g of AP3, and 12.9 g of water were directly transferred to a 50-mL $ZrO_2$ jar containing 102 g of 2-mm diameter $ZrO_2$ grinding balls to be used in a Retsch PM 200 planetary ball mill. The jar was counterbalanced and spun at 500 RPM for 25 h. Immediately after milling, the temperature of the colloid was measured to be 50 °C and the pH was roughly 8.6. The colloid was stored at room temperature and remained in suspension for more than 4 weeks.

### 2.2 Generation of Fluorescent Polymer-Dexamethasone Encapsulated Magnetic Nanoparticles

The materials used to generate fluorescent drug-loaded BaNPs include dexamethasone (Dex, 392.47 M.W.) from Alfa Aesar and MP Biomedicals, LLC; acetone, dichloromethane, polyvinyl alcohol aqueous solution (PVA 0.3 %, 15,000 g/M), acetic acid (0.1 M), sodium hydroxide, hydrogen chloride, methanol, poly(lactic-co-glycolic) acid (PLGA 66,000–107,000 M.W.) with 75:25 lactide/glycolide ratio, fluorescein isothiocyanate (FITC 389.38 M.W.), chitosan (low M.W.), $ddH_20$ (18.2 MΩ/cm), and the AP3-coated BaNPs. The drug, Dex, is a glucocorticoid used to treat various inflammatory and autoimmune conditions [15] and is integrated into the biodegradable PLGA coating [16, 17]. Biocompatible FITC-chitosan was used to tag the drug-coated NPs for confocal microscopy [18].

The fluorescent, drug-coated BaNPs were fabricated in two steps. First, 4 mL of acetone and dichloromethane in a 1:2 ratio (*v*/*v*) was used to dissolve 100 mg (or 50 mg) of PLGA and 10 mg (or 5 mg) of Dex [16, 17] and mixed for a few minutes. One hundred milligrams of AP3-coated NPs (in a 1:1 *w*/*w* ratio with PLGA) suspended in water was transferred to the PLGA-Dex solution and shaken. Then, 12 mL of PVA was added and an emulsion was formed by shaking and ultrasonicating under a sonic tip for 30 s three times with 30-s breaks. After ultrasonication, the emulsion acquired a "milky" look. The emulsion was then added to 50 mL of additional PVA, sonicated again, and stirred overnight to remove organic solvent.

A FITC-chitosan marker was prepared based on the procedures of Ge et al., utilizing the reaction between the isothiocyanate group of FITC and primary amino group of chitosan [18]. A 17.5 mg of FITC was mixed with 20 mL of methanol and added to 20 mL of a 1 % (*w*/*v*) chitosan/0.1 M acetic acid solution (using 0.2 g of chitosan). After 3-h incubation in the dark at room temperature, NaOH was used to raise the pH to 10 and precipitate out the FITC-chitosan. Unreacted FITC was removed by separating the precipitate through centrifugation and washing with water. The FITC-chitosan was then dissolved in 20 mL of 0.1 M acetic acid, shaken, and incubated overnight.

The second step was based on procedures from Ge et al. and Chronopoulou et al. [18, 19]. The PLGA-Dex nanoparticles were washed and prepared in 5 mL of water to obtain a high NP concentration. Half of this colloid was transferred to 20 mL of the FITC-chitosan-acetic acid solution and shaken for 4 h. The supernatant was replaced with 3 mL of water to obtain the FITC-labeled PLGA-Dex NPs in their final form.

As a control, FeNPs were also surface-engineered using the same method (without the milling phase). Twenty to 30 nm $Fe_3O_4$ NPs coated with polyvinylpyrrolidone (PVP) from Nanostructured and Amorphous Materials, Inc., as well as pure 20 nm $Fe_3O_4$ NPs from MTI Corporation were used.

### 2.3 Physical and Magnetic Characterization of Drug-Coated Nanoparticles

Dynamic light scattering (DLS) measurements were performed with a NanoBrook ZetaPALS Zeta Potential Analyzer from Brookhaven Instruments Corporation employing a 35-mW solid state laser (660 nm). A volume of 1 mL of the previously coated and washed particles was transferred to a 1.5-mL centrifuge tube and spun at 11,000 RPM for 1 min keeping the supernatant and discarding the produced pellet. Samples were prepared for measurements by dispersing roughly 0.05 mL of water-suspended AP3-BaNPs (~0.03 g/mL) in a cuvette containing 3.0 mL water. The sample was ultrasonicated with a Branson 200 ultrasonic cleaner for 15 min and immediately placed in the Zeta Potential Analyzer for measurements.

Transmission electron microscopy (TEM) was used to determine the physical characteristics of the BaNPs and FeNPs, as well as the nature of their PLGA-Dex coating. TEM samples were prepared by deposition and drying of 3–5 μL of the NP suspension onto formvar-coated, carbon-evaporated 400-mesh copper grids (FCF400-CU-50, Electron Microscopy Science, Hatfield, PA). High-resolution TEM images were acquired using an FEI Technai G2 BioTwin electron microscope.

Magnetic properties of the NPs were determined using a SQUID magnetometer (Quantum Design MPMS XL). The water-suspended NPs were centrifuged and separated from the supernatant. The remaining water was evaporated under a fume hood at room temperature to obtain the NPs in powdered form. Less than 5 mg of each sample was measured out (taking into account the coating) and were sealed in Kapton tape over a magnet (for alignment of nanoparticles along easy axis) and transferred to the magnetometer. Knowing the mass and density of the BaNPs and FeNPs, a magnetization curve was obtained. Stand-alone Kapton tape was also measured (without the sample) and calibrated out of the final data.

### 2.4 Cell Culturing

NHTE cells were obtained from the tracheas and bronchi of de-identified organ donors whose lungs were not suitable for transplantation as previously described [20]. Collection and the use of these cells were approved by the Institutional Review Board (IRB) at National Jewish Health. Airway epithelial cells at passage 1 were cultured and expanded in collagen-coated 60-mm tissue culture dishes containing bronchial epithelial cell growth medium with supplements (Lonza, Walkersville, MD) at 37 °C, 5 % $CO_2$. At 80 % confluence, they were transferred onto collagen-coated transwell inserts ($4 \times 10^4$ cells/insert) in 12-well plates. After a week in the immersed culture condition, NHTE cells reached 100 % confluence and were shifted to ALI condition by reducing the apical medium volume to 50 μL. ALI conditions were maintained for 10 days because previous studies have demonstrated that culture for 10 days is required for the mucociliary differentiation of human airway epithelial cells [21].

### 2.5 Generation of High Magnetic Field Gradient and Fluorescence Microscopy

Figure 1a shows a schematic of the experimental setup used to apply a magnetic field in the region of the mucus or corn syrup. A permanent Permalloy neodymium (NdFeB) magnet with an iron core pole piece was used to generate a high spatial magnetic field gradient. The decrease of magnetic field as a function of distance from the pole piece was measured using a Lakeshore Mo. 421 Gaussmeter, and the data was used to calculate the spatial magnetic field gradient. Figure 1b depicts the magnetic field strength versus distance from the tip of the pole piece. Briefly, to account for sensor position within the 1.44-mm thick probe of the Gaussmeter, the "tip" of the pole piece was defined to be half of the probe thickness at 0.72 mm. The magnetic field was measured to be 492 ± 5 mT at the tip of the pole piece and about 250 ± 9 mT, 2.5 mm above the tip. At the tip, a maximum gradient of 295 ± 15 T/m was calculated. At 2.5 and 7.5 mm above the tip, the gradient dropped to 60 ± 3 and 12.4 ± 0.7 T/m, respectively. For magnetic field

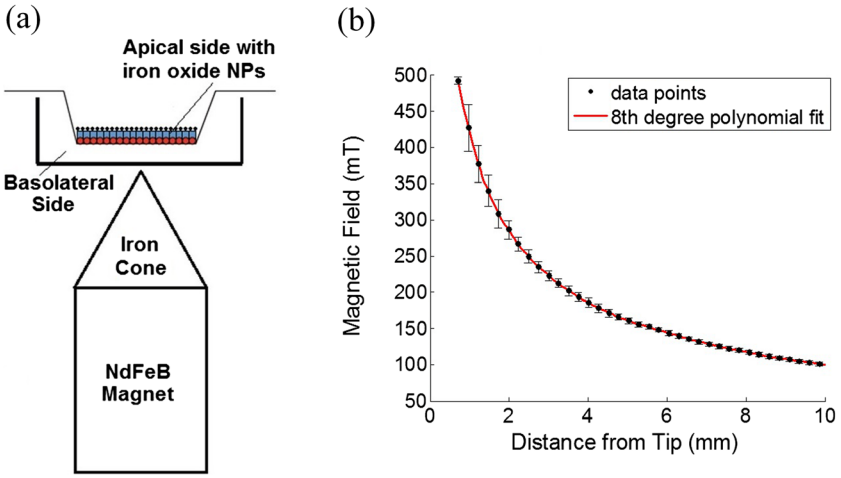


**Fig. 1** **a** Schematic of experimental system to generate and apply focused high magnetic field gradient due to a permanent neodymium (NdFeB) magnet with an iron cone pole piece to primary normal human tracheobronchial epithelial (NHTE) cells. NHTE cells are depicted in *red* and mucus layer is depicted in *blue*. The apical side mimics the airway lumen and the basolateral side mimics the airway submucosa. **b** Magnetic field amplitude (**b**) versus distance (*z*) from the tip of the pole piece. Data points (*black*), representing the mean of three measurements, were phenomenologically fit to an eighth degree polynomial (*solid red line*) from which the magnetic field gradient (dB/dz) was calculated. *Error bars* represent the standard error of three measurements (color figure online)

measurements at different distances above the tip (*z*-positions), the probe was attached to a micrometer stage, initially touching the tip of the magnet. The magnetic field measurement for each z-position was maximized by *x*-*y* plane adjustment of the sensor. Triplicate measurements in the *z*-direction were taken in 50.8-μm increments up to 10 mm above the tip. An eighth degree polynomial was phenomenologically fit to the mean magnetic field amplitude (B). The obtained polynomial was then used to calculate the magnetic field gradient (dB/dz).

The colloid under study was added directly to the top of a ~5-mm thick layer of corn syrup (7.5 mm above the magnet tip) filled in a 12-well plate or on a 100-μm thick mucus layer (2.5 mm above the tip) produced by an ALI NHTE cell culture. To pull magnetic NPs through the corn syrup or mucus layer, the tip of the pole piece was positioned in the center of one well of the 12-well plate. The sample was exposed to a high magnetic field gradient for up to 1 h in 10-min increments. In between field gradient exposures, the 12-well plate containing corn syrup or the transwell inserts with NHTE cells placed on top of a 0.17-mm cover glass was moved to a Leica TCS SP5 confocal laser scanning microscope to determine magnetic NP penetration depth as a function of magnetic pulling time. Bright field and fluorescence images were collected with a ×40 oil immersion objective (NHTE cells) or ×20 objective (corn syrup) at room temperature. The confocal pinhole was set to one airy unit and the z-step size was set to 2.3 and 1.6 μm for the ×20 and ×40 objective, respectively. FITC-labeled magnetic NPs were excited with 488-nm laser light. To monitor the fluorescence and the NPs, an emission detection range from 505 to 680 nm together with 488/543-nm dichroic filter (beam splitter) was applied.

## 3 Results and Discussion

### 3.1 Size Characterization of Milled BaNPs via Dynamic Light Scattering

Average particle diameter and size distribution of the AP3-coated BaNPs after milling were determined using DLS. A fixed scattering angle of 90° relative to the incident beam of 660 nm was held, while measurements were averaged over five to six runs totaling 15–18 min. The refractive index of the BaNPs [22], not taking into account the surfactant layer, is $n = 2.8 + i(0.12)$ and was used by the software of the Zeta Potential Analyzer to determine particle size. Various batches of BaNPs with diameters in the range of 1–100 nm were milled. Figure 2 shows the number (Fig. 2a) and intensity-weighted (Fig. 2b) size distributions of AP3-coated BaNPs after 25 h of milling. In this sample, the mode and mean diameters were 34.1 and 36.4 nm, respectively. The BaNPs had a narrow size distribution from 34.1 to 38.8 nm. A small portion (<1 % by number) of large particles (144 nm in mean diameter) was also present and is depicted in Fig. 2b. These larger particles can be removed through centrifugation as described above.

### 3.2 Transmission Electron Microscopy Images of Drug-Coated Magnetic Nanoparticles

TEM images of the PLGA-Dex-coated BaNPs and FeNPs were taken to understand their physical characteristics (Fig. 3). If the PLGA layer around the NPs is too thick, or if the NPs are bonded to micrometer-sized agglomerates of PLGA, then particle motion through the mucus will be

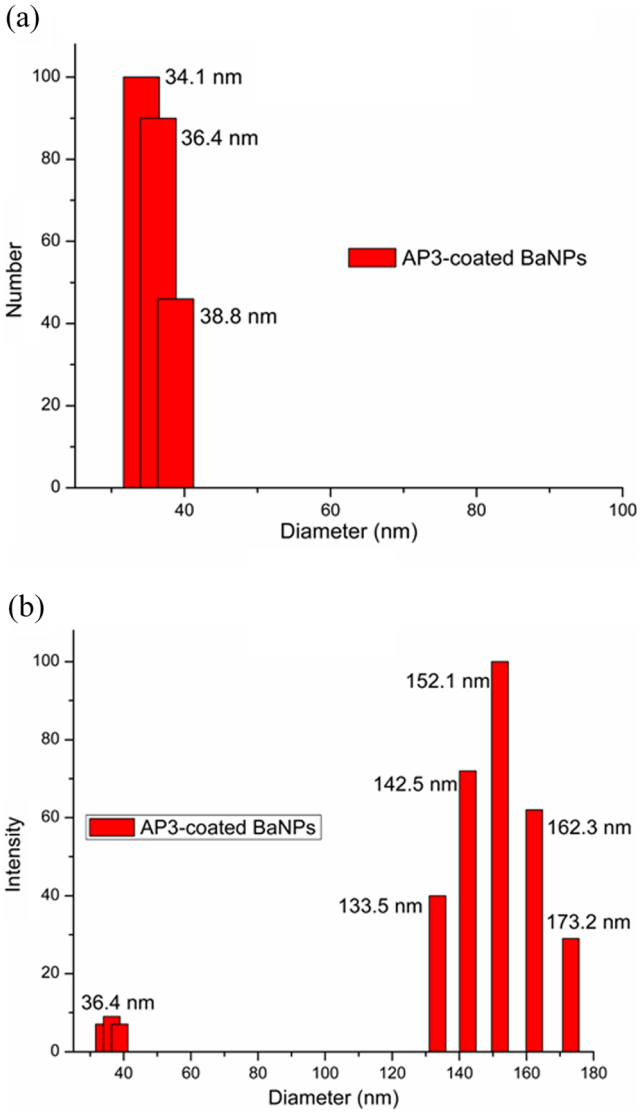


**Fig. 2** **a** Number-weighted size distribution of milled AP3-BaNPs. The majority of NPs were 34.1 nm in diameter. **b** Intensity-weighted size distribution of milled AP3-BaNPs. A small portion (<1 % by number) of NPs ranged from 133.5- to 173.2-nm diameter

impeded. The primary reason for this is that the mucus structure is composed of cross-linked mucin fibers enclosing pores ranging from ~100 nm to several micrometers in diameter [10]; therefore, the PLGA-Dex NPs may have to be relatively small to achieve effective penetration.

To obtain a thinner coating of PLGA around the NPs and/or obtain smaller PLGA globules in the final colloid, NPs were fabricated with less PLGA in the second production of the nanomedicine (50 mg of PLGA vs. 100 mg). As seen in Fig. 3, isolated PLGA-Dex NPs as well as agglomerates of NPs bonded to small PLGA-Dex globules are evident. These particles (with reduced polymer coating) were shown to have greater mobility in the mucus structure and corn syrup model, to be discussed below. Finally, we note in Fig. 3c the general shape of the PLGA-DexBaNPs. These particles are noticeably rod-shaped and therefore have a different shape anisotropy than the spherical FeNPs.

### 3.3 Mobility of Nanoparticles in Corn Syrup Under High Gradient Magnetic Field

Initially, various particles were tested for their ability to penetrate a ~5-mm thick layer of corn syrup, which is an inexpensive model for mucus. The dynamic viscosity for corn syrup is about 20 Pa/s which is similar to the viscosity for human respiratory mucus in the range of 12–15 Pa/s [23]. We note that pulmonary disease conditions, such as cystic fibrosis, COPD, and asthma, generally result in an increase in the viscoelasticity of mucus, owing in part to reduced water content and an increased fraction of glycoproteins [23]. Approximately 30 mg/mL of uncoated $BaFe_{12}O_{19}$ NPs (500 nm), AP3-BaNPs (34 nm), uncoated $Fe_3O_4$ NPs (20 nm), and PVP-$Fe_3O_4$ NPs (20–30 nm) suspended in water were transferred to the top surface layer of the syrup and allowed to settle. Uncoated $Fe_3O_4$ and $BaFe_{12}O_{19}$ NPs were shown to sink readily with gravity through the syrup within 5–10 min. However, the AP3-coated BaNPs (34 nm) and PVP-coated $Fe_3O_4$ NPs sank at a slower rate through the syrup (~15 and 1–2 h, respectively).

The same set of particles was also tested for their mobility through corn syrup as a magnetic field gradient of $12.4 \pm 0.7$ T/m was applied to the top of the corn syrup a distance of 7.5 mm above the tip. All particles except AP3-BaNPs penetrated the syrup in seconds, with the latter taking 1–2 h to penetrate. Although the time for the AP3-BaNPs was reduced substantially by adding a magnet, they moved relatively slowly, which we attribute primarily to

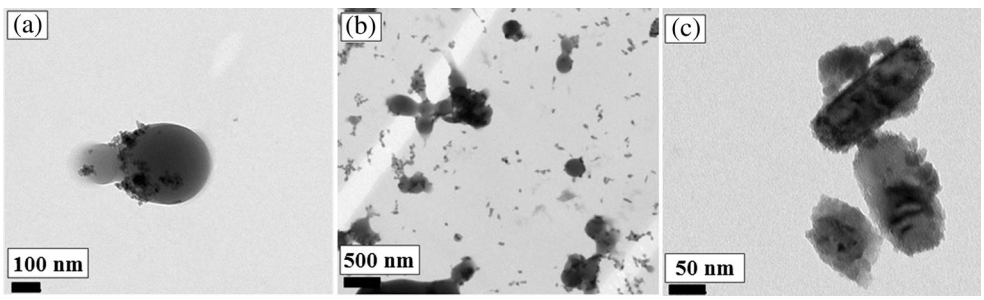


**Fig. 3** TEM image of **a** $Fe_3O_4$ nanosphere agglomerates bonded to a PLGA-Dex globule. NPs are visible as *dark spots* on a larger, gray PLGA globule, **b** AP3-BaNPs and agglomerates coated and/or bonded with PLGA-Dex globules, and (**c**) 50-nm scale PLGA-Dex-coated BaNPs in the shape of platelets with hexagonal base

the reduced magnetic response of the milled particles (discussed in a later section).

Studies were then performed on the mobility of PLGA-Dex BaNPs and FeNPs (both made with 100 mg of PLGA) in corn syrup. The fluorescent PLGA-Dex FeNPs were pulled through corn syrup via magnet within 30 min, slightly longer than the uncoated particles. The fluorescent PLGA-Dex BaNPs took roughly 24 h. This result was brought to within 30 min by reducing the quantity of PLGA to 50 mg during the production process. The diameter of these PLGA globules ranged from approximately 100 nm to a few microns (see Fig. 3b). This is a broad size distribution and is consequently difficult to characterize. In future studies, the fluorescent drug-loaded polymer coating protocol will be redefined to obtain approximately 100 nm PLGA-Dex NPs with a narrow size distribution.

### 3.4 SQUID Magnetometry of FeNPs and BaNPs

Figure 4 shows the magnetization versus applied magnetic field of uncoated 500 nm BaNPs (black squares), 20–30 nm FeNPs (red closed circles), and ~34 nm milled AP3-BaNPs (blue triangles) measured with a SQUID magnetometer. The milled BaNPs had substantially lower saturation magnetization than the other NPs. The magnetization curve shape also suggests that both paramagnetic and ferromagnetic phases are present in the sample. This result explains the reduced mobility of milled particles through corn syrup. We speculate that a portion of the $BaFe_{12}O_{19}$ is undergoing a chemical change during the milling process (e.g., to $BaCO_3$, etc.) [13]. One potential solution to maintaining the composition and magnetic properties of $BaFe_{12}O_{19}$ during NP production is to mechanically crush the NPs (versus wet milling). This will be addressed in a future study.

### 3.5 Mobility of Drug-Loaded Magnetic Nanoparticles Through Mucus Under High Gradient Magnetic Field

To test the efficiency of the conventional FeNPs (20–30-nm diameter) in higher field gradients, 100 μg/mL PVP-coated FeNPs were added on top of a mucus layer of NHTE cells. The cells were exposed to a magnetic field gradient of 60 ± 3 T/m for 1 h (Fig. 1a). Figure 5a shows a bright field image of the in-focus NHTE cells (gray) and PVP-coated 30-nm $Fe_3O_4$ NP aggregates. In our high magnetic flux delivery system, FeNPs successfully penetrated the ~100-μm thick mucus layer and reached the epithelial cells (particles and cells are in focus). Out-of-focus FeNPs have not yet reached the cell layer (as determined by confocal *z*-sections, Fig. 5b). It is apparent from these experiments that FeNPs can reach the cell layer when exposed to high field gradients. Here, particles tend to form clumps and do not coat the cell layer uniformly. Thus, the current experimental system lacks the uniform coverage that is critical for efficient drug delivery.

To test the efficiency of newly generated FITC-labeled Dex-BaNPs, 100 μg/mL of the NPs was added on top of the mucus layer of NHTE cells. Using the experimental setup shown in Fig. 1a, the cells were exposed to a high magnetic field gradient of 60 ± 3 T/m for 10, 20, and 30 min. At each time point, confocal *z*-sections of drug-loaded NP penetrating the mucus layer were collected. The *z*-step size was set to 940 nm. Figure 6a depicts the normalized fluorescent intensity of FITC-labeled Dex-BaNPs at different distances (mucus z-sections) from the NHTE cell layer after 10 min

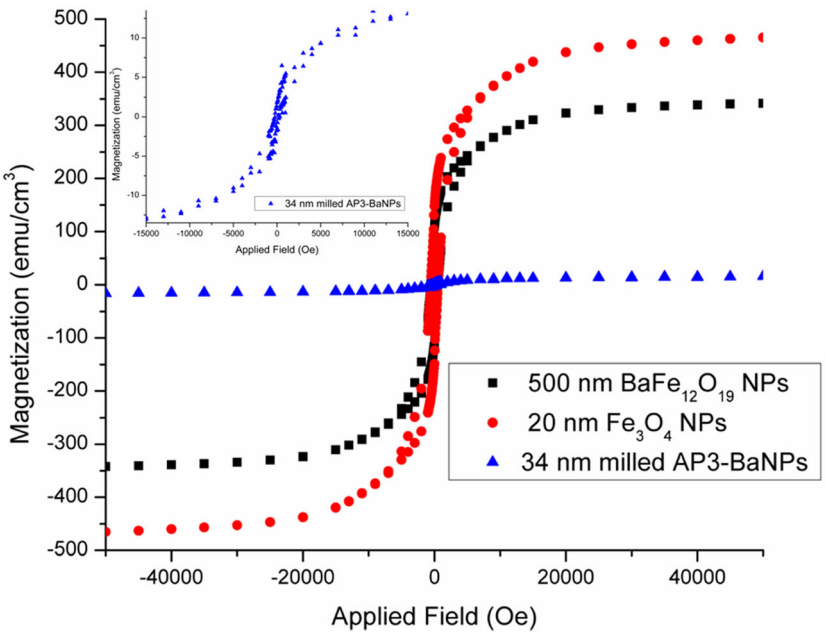


**Fig. 4** SQUID magnetometry measurements of 500-nm BaNPs (*black squares*), 20–30-nm FeNPs (*red closed circles*), and ~34-nm milled AP3-BaNPs (*blue triangles*). The *inset* shows a zoomed-in graph of the hysteresis curve for the milled AP3-BaNPs

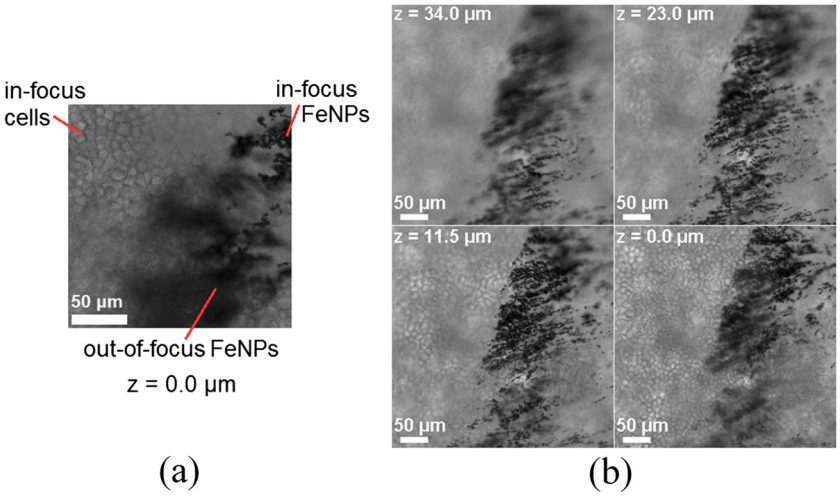


**Fig. 5** Bright field image of primary human airway epithelial cells (*gray*) and PVP coated 20–30-nm $Fe_3O_4$ magnetic nanoparticle (FeNP) aggregates (*black*). The sample was exposed to a magnetic field gradient of 60 ± 3 T/m for 1 h. **a** Some FeNPs (in-focus FeNPs) successfully penetrated the 100-μm thick mucus and reached the cell layer at $z = 0.0$ μm. **b** A confocal *z*-stack montage of individual confocal *z*-slices. When FeNPs reached the cell layer, both NPs and cells are in focus ($z = 0.0$ μm). NPs that are in-focus at $z = 11.5$, 23.0, and 34.0 μm did not reach the cell layer. The *scale bar* represents 50 μm

(blue triangles), 20 min (red circles), and 30 min (black solid line). Figure 6a shows the amount of FITC-labeled Dex-BaNPs reaching the NHTE cell layer increases with increasing magnetic field exposure as the peak of the distribution shifts toward the left (toward the NHTE cell layer). Moreover, an increased peak and decreased width of the distribution as a function of magnetic field exposure time indicate that a larger number of FITC-labeled Dex-BaNPs reached the NHTE cell layer over time. The majority of fluorescent Dex-BaNPs reached the top of the NHTE cell layer when exposed to high field gradients within 30 min; see Fig. 6b. Similar to FeNPs, FITC-labeled Dex-BaNPs also tend to form clumps and do not coat the cell layer uniformly (data not shown).

### 3.6 Bioactivity of Dex-BaNPs

To determine the bioactivity of Dex-BaNPs, we performed a pilot lung epithelial cell line (NCI-H292) culture by treating the cells with Dex-BaNPs (Dex concentration, $10^{-7}$ M), Dex alone (no BaNPs), or BaNPs alone (no Dex) for 24 h in the presence or absence of a TLR2 agonist Pam2CSK4 (100 ng/ml). Pam2CSK4 is known to induce mucins and pro-inflammatory cytokines (e.g., IL-8) [24, 25]. First, Dex-BaNPs as well as FeNPs did not have any cytotoxic effects as indicated by similar lactate dehydrogenase (LDH) levels measured using the LDH assay kit (Pierce Biotechnology, Inc.) in supernatants of cells with or without BaNP treatment. Dex-BaNPs (no cytotoxicity) were 80 and 85 % as effective as Dex

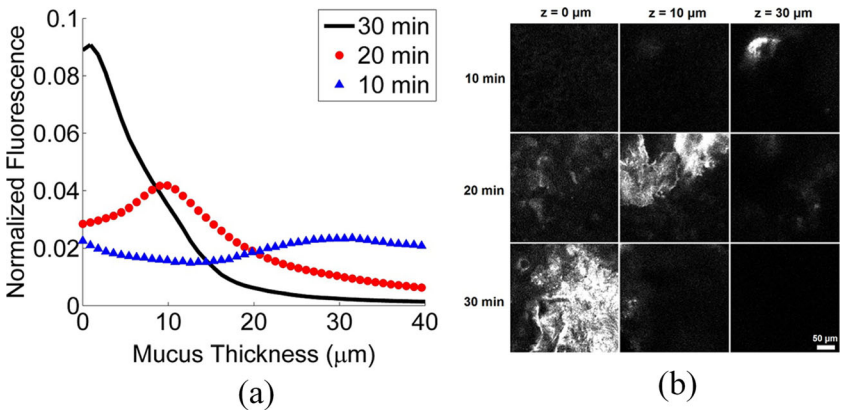


**Fig. 6** **a** Normalized fluorescent intensity of FITC-labeled PLGA-Dex BaNPs at different mucus *z*-sections after 10 min (*blue triangles*), 20 min (*red circles*), and 30 min (*black solid line*) exposure to a high magnetic field gradient of 60 ± 3 T/m. The *z*-position of the top of the NHTE cell layer is represented by a mucus thickness of 0 μm. **b** A confocal *z*-stack montage of individual confocal *z*-slices. *Top row*, *middle row*, and *bottom row* represent fluorescent images of FITC-labeled PLGA-Dex BaNPs after 10-, 20-, and 30-min exposure to a high magnetic field gradient, respectively. *First column*, *second column*, and *third column* represent the corresponding images at different *z*-positions. All images have the same brightness scale and the *scale bar* represents 50 μm

alone in inhibiting Pam2CSK4-induced mucin MUC5AC expression and IL-8 production, respectively. This result suggests that 80 to 85 % of DEX were released from PLGA into the aqueous solution from the time of drug-coated NP preparation to the end of the 24-h study. This result is consistent with a previously published release study [17]. Of note, BaNPs alone did not have any effects on Pam2CSK4-induced MUC5AC and IL-8.

## 4 Conclusion

A permanent magnet producing a high magnetic field gradient of 295 ± 15 T/m at the tip of the pole piece was used to pull drug-loaded NPs through a ~100-μm thick mucus layer of air-liquid interface cultured primary NHTE cells within the clearance time of 1 h. Both $Fe_3O_4$ and $BaFe_{12}O_{19}$ NPs were encapsulated with PLGA containing dexamethasone and suspended in water. The particles were introduced to the surface of mucus and allowed to settle by the magnetic field gradient. The size distribution and average diameter of ~35 nm for non-PLGA-coated $BaFe_{12}O_{19}$ NPs were determined by dynamic light scattering. Transmission electron microscopy revealed shape anisotropy of the $BaFe_{12}O_{19}$ particles and indicated that agglomerates of NPs are bonded to larger PLGA globules ranging from 100 nm to a few microns in size. SQUID revealed the magnetic properties of the particles lending explanation to the slow mobility of the milled BaNPs. Nanoparticle clearance through mucus was accomplished by applying a high magnetic field gradient of 60 ± 3 T/m at a distance of 2.5 mm above the tip and was enhanced by optimizing the quantity of PLGA used for coating.

**Acknowledgments** This work was in part supported by the Center for the Biofrontiers Institute, University of Colorado at Colorado Springs, the Colorado Bioscience Discovery Evaluation Grant Program to Hong Wei Chu, and by the grants from the National Institutes of Health to Hong Wei Chu: R01 HL122321, R01 AI106287 and R01 HL125128. The authors thank Dorothy Dill (Electron Microscopy Center, University of Colorado Denver) for assistance with TEM, Joshua Baptist for magnet assembly, and useful discussion with Dr. Robert Camley, Dr. Ke Jiang, William Townend, and Kyle Culhane.

## References

1. Hauber, H. P., Steffen, A., et al. (2008). Effect of steroids, acetylcysteine and calcium-activated chloride channel inhibitors on allergic mucin expression in sinus mucosa. *Laryngoscope, 118*, 1528–1533.
2. Riesenfeld, E. P., Sullivan, M. J., et al. (2010). Inhaled salmeterol and/or fluticasone alters structure/function in a murine model of allergic airways disease. *Resp Res, 11*, 22.
3. Groneberg, D. A., Eynott, P. R., et al. (2002). Expression of respiratory mucins in fatal status asthmaticus and mild asthma. *Histopathology, 40*, 367–373.
4. Ensign, L. M., Tang, B. C., et al. (2012). Mucus-penetrating nanoparticles for vaginal drug delivery protect against herpes simplex virus. *Science Translational Medicine, 4*, 138.
5. Rytting, E., Nguyen, J., et al. (2008). Biodegradable polymeric nanocarriers for pulmonary drug delivery. *Expert Opin Drug Del, 5*, 629–639.
6. Lai, S. K., Wang, Y. Y., Hanes, J. (2009). Mucus-penetrating nanoparticles for drug and gene delivery to mucosal tissues. *Adv Drug Deliver Rev, 61*, 158–171.
7. Morgan, L., Pearson, M., et al. (2004). Scintigraphic measurement of tracheal mucus velocity in vivo. *European Respiratory Journal, 23*, 518–522.
8. McGill, S. L., Cuylear, C. L., et al. (2009). Magnetically responsive nanoparticles for drug delivery applications using low magnetic field strengths. *IEEE T NanoBioSci, 8*, 33–42.
9. Ally, J., Roa, W., Amirfazli, A. (2008). Use of mucolytics to enhance magnetic particle retention at a model airway surface. *Journal of Magnetism and Magnetic Materials, 320*, 1834–1843.
10. Kirch, J., Schneider, A., et al. (2012). Optical tweezers reveal relationship between microstructure and nanoparticle penetration of pulmonary mucus. *P Natl Acad Sci USA, 109*, 18355–18360.
11. Dames, P., Gleich, B., et al. (2007). Targeted delivery of magnetic aerosol droplets to the lung. *Nature Nanotechnology, 2*, 495–499.
12. Hergt, R., Dutz, S., & Zeisberger, M. (2010). Validity limits of the Neel relaxation model of magnetic nanoparticles for hyperthermia. Nanotechnology, 21, 015706. doi: 10.1088/0957-4484/21/1/015706.
13. Kaczmarek, W. A., & Ninham, B. W. (1995). Surfactant-assisted ball milling of BaFe12O19 ferrite dispersion. *Materials Chemistry and Physics, 40*, 21–29.
14. Liu, L. H., & Mingdi, Y. (2010). Perfluorophenyl azides: new applications in surface functionalization and nanomaterial synthesis. *Accounts Chem Res, 43*, 1434–1443.
15. Brouwer, M. C., McIntyre, P., et al. (2013). Corticosteroids for acute bacterial meningitis. Cochrane Db Syst Rev, 6, CD004405. doi: 10.1002/14651858.CD004405.pub4.
16. Verma, N. K., Crosbie-Staunton, K., et al. (2013). Magnetic core-shell nanoparticles for drug delivery by nebulization. J Nanobiotechnology, 11:1. doi: 10.1186/1477-3155-11-1.
17. Gomez-Gaete, C., Tsapis, N., et al. (2007). Encapsulation of dexamethasone into biodegradable polymeric nanoparticles. *International Journal of Pharmaceutics, 331*, 153–159.
18. Ge, Y., Zhang, Y., et al. (2009). Fluorescence modified chitosan-coated magnetic nanoparticles for high-efficient cellular imaging. *Nanoscale Research Letters, 4*, 287–295.
19. Chronopoulou, L., Massimi, M., et al. (2013). Chitosan-coated PLGA nanoparticles: a sustained drug release strategy for cell cultures. *Colloid Surface B, 103*, 307–310.
20. Wu, Q., Jiang, D., et al. (2012). IL-13 dampens human airway epithelial innate immunity through induction of IL-1 receptor-associated kinase M. *J Allergy Clin Immun, 129*, 825–833.
21. Chu, H. W., Balzar, S., et al. (2004). Transforming growth factor-β2 induces bronchial epithelial mucin expression in asthma. *American Journal of Pathology, 165*, 1097–1106.
22. Harward, I., Nie, Y., et al. (2013). Physical properties of Al doped Ba hexagonal ferrite thin films. J Appl Phys, 113, 043903. doi: 10.1063/1.4788699.
23. Lai, S. K., Wang, Y. Y., et al. (2009). Micro- and macrorheology of mucus. *Adv Drug Deliver Rev, 61*, 86–100.
24. Evans, S. E., Xu, Y., et al. (2010). Inducible innate resistance of lung epithelium to infection. *Annual Review of Physiology, 72*, 413–435.
25. Chu, H. W., Jeyaseelan, S., et al. (2005). TLR2 signaling is critical for Mycoplasma pneumoniae-induced airway mucin expression. *Journal of Immunology, 174*, 5713–5719.